Development/Plasticity/Repair

Nerve Growth Factor Regulates the Firing Patterns and Synaptic Composition of Motoneurons

María A. Davis-López de Carrizosa,* Camilo J. Morado-Díaz,* Sara Morcuende, Rosa R. de la Cruz, and Ángel M. Pastor

Departamento de Fisiología y Zoología, Facultad de Biología, Universidad de Sevilla, 41012 Sevilla, Spain

Target-derived neurotrophins exert powerful synaptotrophic actions in the adult brain and are involved in the regulation of different forms of synaptic plasticity. Target disconnection produces a profound synaptic stripping due to the lack of trophic support. Consequently, target reinnervation leads to synaptic remodeling and restoration of cellular functions. Extraocular motoneurons are unique in that they normally express the TrkA neurotrophin receptor in the adult, a feature not seen in other cranial or spinal motoneurons, except after lesions such as axotomy or in neurodegenerative diseases like amyotrophic lateral sclerosis. We investigated the effects of nerve growth factor (NGF) by retrogradely delivering this neurotrophin to abducens motoneurons of adult cats. Axotomy reduced the density of somatic boutons and the overall tonic and phasic firing modulation. Treatment with NGF restored synaptic inputs and firing modulation in axotomized motoneurons. When K252a, a selective inhibitor of tyrosine kinase activity, was applied to specifically test TrkA effects, the NGF-mediated restoration of synapses and firing-related parameters was abolished. Discharge variability and recruitment threshold were, however, increased by NGF compared with control or axotomized motoneurons. Interestingly, these parameters returned to normal following application of REX, an antibody raised against neurotrophin receptor p75 (p75^{NTR}). In conclusion, NGF, acting retrogradely through TrkA receptors, supports afferent boutons and regulates the burst and tonic signals correlated with eye movements. On the other hand, p75^{NTR} activation regulates recruitment threshold, which impacts on firing regularity. To our knowledge, this is the first report showing powerful synaptotrophic effects of NGF on motoneurons *in vivo*.

Introduction

In the adult brain, neurotrophins modulate a variety of functions, from regeneration to myelination and from pain to depression. Frequently, these actions involve synaptic reorganizations (McAllister et al., 1999). This synaptotrophic role of neurotrophins results in changes in the balance between excitation and inhibition and in the number and activity of synapses (Singh et al., 2006; Huh et al., 2008). Moreover, neurotrophins have a role regulating discharge properties at the cellular and network levels (Berardi et al., 2003; Caleo et al., 2003; Luther and Birren, 2009). However, given the multiplicity of pathways and signaling events in the brain, combined with its heterogeneous synaptic organization, no common rule for neurotrophin action emerges that could apply to every part of the brain. Therefore, an *in vivo* approach is also needed to unravel the actions of neurotrophins under physiological and pathological conditions (Chao, 2003).

Received Feb. 8, 2010; revised April 29, 2010; accepted May 7, 2010.

This work was supported by MCYT-FEDER Grants BFU2009-07121 and PET2008-0226, Fundación Eugenio Rodríguez Pascual, and Junta de Andalucía (P06-CTS-01420 and P09-CVI-4617). M.A.D.-L.C. was a scholar of the FISS in Spain. Some experiments were performed in the Imaging and Biology central services (CITIUS). We thank Dr. Louis Reichardt, University of California, San Francisco, for generously providing the REX antibody. We also thank Dr. Francisco Alvarez, Wright State University, for critical reading of the manuscript.

*M.A.D.-L.C. and C.J.M.-D. contributed equally to this work.

Correspondence should be addressed to Dr. Angel M. Pastor, Departamento de Fisiología y Zoología, Facultad de Biología, Avenida Reina Mercedes 6, 41012 Sevilla, Spain. E-mail: ampastor@us.es.

DOI:10.1523/JNEUROSCI.0719-10.2010

 0270-6474/10/308308-12$15.00/0

Extraocular motoneurons express TrkA, the high affinity receptor for nerve growth factor (NGF) (Benítez-Temiño et al., 2004). In contrast, other cranial and spinal motoneurons only express it transiently during development. Interestingly, the TrkA receptor reappears in spinal motoneurons after lesion or in response to pathologies such as amyotrophic lateral sclerosis (ALS), a disease that spares extraocular motoneurons (Obál et al., 2006; Ferrucci et al., 2010). In this case, surviving motoneurons switch their neurotrophin expression from brain-derived neurotrophic factor (BDNF) and neurotrophin-3 (NT-3) to NGF (Nishio et al., 1998). NGF is expressed in developing skeletal muscle, but is downregulated in the adult (Ebendal et al., 1986; Ernfors et al., 1991; Koliatsos et al., 1993; Ip et al., 2001) and upregulated during muscle repair (Deponti et al., 2009) or in response to musculoskeletal pathologies (Küst et al., 2002; Toti et al., 2003). The action of NGF in extraocular motoneurons and reasons for persistence of NGF neurotrophic responses into adulthood are unclear.

Decreased retrograde trophic support after peripheral nerve injury leads to profound synaptic stripping of motoneuron membranes that reduces responsiveness to afferent signals (de la Cruz et al., 1996). These alterations revert to normal following reinnervation of natural or exogenous targets (Delgado-García et al., 1988; Benítez-Temiño et al., 2005) or when BDNF and NT-3 are exogenously applied (Davis-López de Carrizosa et al., 2009). A possible role for NGF in regulating the morphophysiological characteristics of extraocular motoneurons and its afferent inputs has not yet been studied. To analyze this possibility, we induced alterations in the levels of NGF by either axotomy or

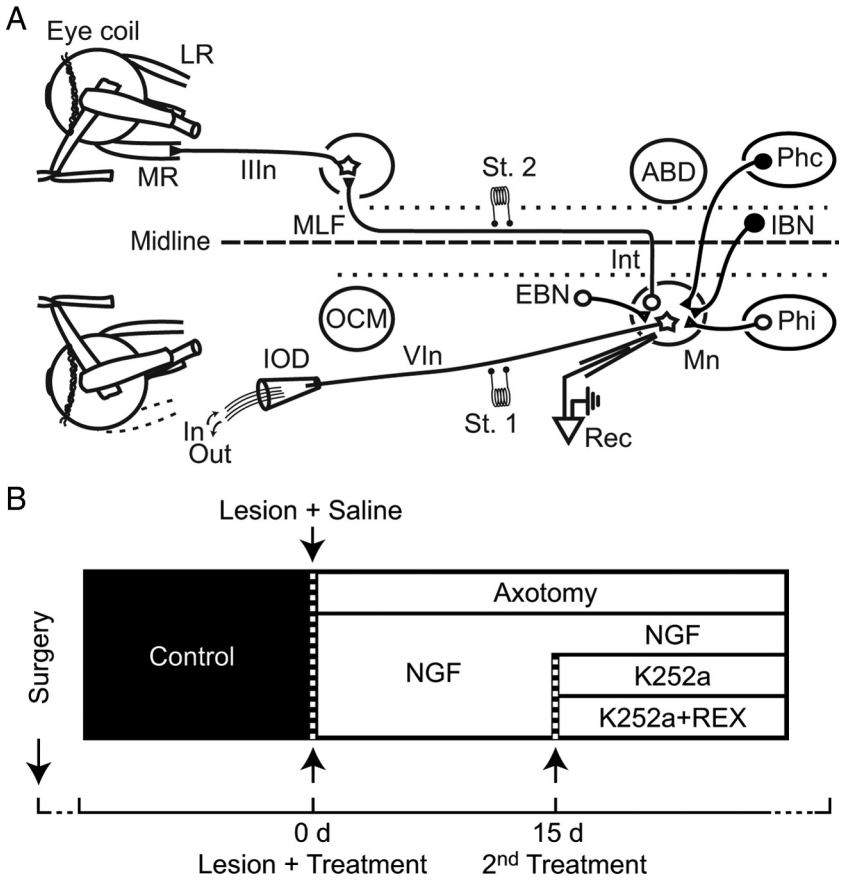

Figure 1. ***A***, Diagram of the experimental design for single-unit and eye movement recordings (Rec). The abducens nucleus (ABD) contains motoneurons (Mn), which innervate the lateral rectus muscle (LR), and internuclear neurons (Int), which has axons that contact the contralateral medial rectus muscle (MR) innervating motoneurons through the oculomotor nerve (IIIn) of the oculomotor nucleus (OCM). Abducens neurons receive burst input from excitatory (EBN) and inhibitory (IBN) reticular neurons, and tonic inputs from bilaterally (i, ipsilateral; c, contralateral) projecting prepositus hypoglossi (Ph) neurons. Bipolar stimulating (St.) electrodes were implanted on the VIth nerve (VIn; St. 1) and on the medial longitudinal fasciculus (MLF; St. 2). After control sessions, the lateral rectus muscle was removed and an intraorbitary device (IOD) was implanted in the VIth nerve. ***B***, Diagram of the time course of treatments.

externally applying NGF to the stump of the sectioned nerve (Davis-López de Carrizosa et al., 2008). Then, we examined the actions of NGF through its two receptors, neurotrophin receptor p75 ($p75^{NTR}$) and TrkA. Our data show that NGF has powerful synaptotrophic effects on excitatory and inhibitory synaptic inputs to motoneurons that control firing patterns and discharge characteristics.

Materials and Methods

Animals and surgical procedures. Experiments were performed on adult female cats weighing 2.0–2.5 kg obtained from authorized suppliers (Servicio de Animales de Experimentación, Universidad de Córdoba, Córdoba, Spain). Animals were surgically prepared for chronic recording of eye movements and neuronal extracellular recordings in the abducens nucleus ($n = 6$) or for histological purposes ($n = 6$). The latter were just instrumented for chronic supply of NGF. Surgical and handling procedures for chronic experiments were in compliance with current legislation (R.D. 120/2005 BOE 252/34367-91, 2005).

Animals instrumented for chronic recordings received a vagolytic injection of atropine sulfate (0.5 mg/kg, i.m.) and were then anesthetized with sodium pentobarbital (35 mg/kg, i.p.) and positioned in a stereotaxic frame to implant bipolar stimulating electrodes in the abducens nerve and the medial longitudinal fasciculus to antidromically activate abducens motoneurons and interneurons, respectively (Fig. 1*A*). Coils, made up of two turns of Teflon-insulated stainless-steel wire, were implanted in the sclera of both eyes. A recording chamber made of acrylic resin was constructed over a squared window (5 mm per side) drilled in the occipital bone to allow the transcerebellar passage of recording micropipettes. Finally, a pedestal made of dental acrylic with embedded bolts was constructed to immobilize the head during the recordings.

Postoperative and continuous care. Postoperative care was provided daily throughout the experiment. During the initial 3 d, antibiotics (streptomycin and penicillin, 20.000 I.U./kg, i.m.), and analgesics (pirazolone, 0.1 g/kg, i.m.) were administered. The eyes and the skin around the implanted sockets were also inspected daily and cleaned if needed with sterile saline. During the postoperative period, the animal was adapted to the restraining system for periods of 20 min during the aseptic cleansing of the recording chamber with sterile saline and instillation with drops of antibiotics (0.3% gentamicin sulfate) and calibration of eye movements. For closure of the chamber, the cerebellar surface was protected with a silicone sheath and the chamber sealed with aseptic gauze and a cap.

Chronic recordings. Control recording sessions started after 2 weeks of postoperative recovery. The animal was gently restrained in a fabric bag, wrapped with elastic bandages, and placed in a Plexiglas cradle inside the magnetic field search coil (Fuchs and Robinson, 1966). Extracellular recordings were performed with glass micropipettes pulled with long shanks (30 mm) and tips beveled to a resistance of 1–2 MΩ when filled with 2 M NaCl. The left abducens nucleus was located with the aid of the antidromic field potential produced by electrical stimulation of the VIth nerve. The extracellular neuronal activity was amplified and filtered at a bandwidth of 10 Hz–10 kHz for display and digitalization purposes.

Data storage and analysis. Horizontal and vertical eye position of both eyes and associated neuronal activity were digitally stored for off-line analysis (Power 1401, Cambridge Electronic Design). Computer programs written in Matlab 6.5 displayed instantaneous firing frequency (i.e., the reciprocal of the interval between two adjacent spikes) and the position of both eyes for the purpose of data selection. Relationships between neuronal firing rate (FR) [in spikes/s (sp/s)] and horizontal eye position (EP) [in degrees (deg)] were obtained by linear regression analysis to calculate the slope, i.e., the neuronal sensitivity to eye position (k, in sp/s/deg), the ordinate intercept (F_0, in sp/s), and the abscissa intercept (the recruitment threshold, in deg). Firing rate during fixations was represented by the equation $FR = k \times EP + F_0$. Relationships between neuronal firing and eye velocity during saccades were obtained by linear regression after subtraction of the position component ($k \times EP$) calculated from the previously known sensitivity to eye position. Thus, the equation used was $FR - k \times EP = r \times EV + F_0$, where r (in sp/s/deg/s) is the neuronal sensitivity to eye velocity (EV) (in deg/s). Due to the impairment of eye movements of the affected eye, we used the noninjected, contralateral eye for computation of eye movements.

Abducens nerve section and preparation of the implantable intraorbitary device. For the delivery of NGF or inhibitors of NGF receptors, we implanted the stump of the abducens nerve in a custom-made suction chamber that allowed the control of the extracellular environment that bathed the nerve stump. This also prevented axonal reinnervation of extraocular muscles or any other structure (Baker et al., 1981; Delgado-García et al., 1988). This so-called intraorbitary device consisted of a chamber with two pieces of tubing inserted for the push–pull of fluid

(Davis-López de Carrizosa et al., 2008). The chamber was made with a standard polypropylene pipette tip shortened to ~15 mm, thus giving it a conical shape. The wider side of the cone contained the tips of two 6-cm-long pieces of thin-wall polytetrafluoroethylene (PTFE) capillary (26 gauge, Small Parts). The tubing was glued in place to the wide side of the chamber. The narrow part of the conical chamber was left open, ~1 mm wide, to tightly fit the stump of the abducens nerve. After a few control recording sessions to locate the abducens nucleus, the intraorbitary device was implanted under general anesthesia (dose as above) in a second surgical step. The eye was approached temporally through a skin incision over the zygomatic arch. The abducens nerve was dissected free and the lateral rectus muscle removed. The nerve stump was inserted in the chamber by applying suction through the tubing system. The tubing was passed under the skin and was connected into a capped plastic chamber affixed to the head restraint system with dental acrylic.

Administration of NGF and the inhibitors K252a and REX. The protocol for NGF (Sigma) delivery consisted of single injections of 15 μl of a 100 ng/μl solution in saline into the nerve chamber. These were delivered on alternate days over a period of 4–6 weeks (Fig. 1*B*). NGF, with or without the different inhibitors, was delivered during the recording session after rinsing the chamber thoroughly with sterile saline. The concentration used was similar to those used in other *in vivo* studies (Villa et al., 1996; Pizzorusso et al., 1999). K252a, a selective inhibitor of tyrosine protein kinase activity (Rutherford et al., 1997; Rattiner et al., 2004; Bozdagi et al., 2008), was delivered at 100 nM in saline with 2% dimethylsulfoxide mixed with NGF (Tapley et al., 1992). To block $p75^{NTR}$ activity, the polyclonal antibody against the rat extracellular domain of $p75^{NTR}$ (referred to as REX; Weskamp and Reichardt, 1991) was injected at a final concentration of 200 μg/μl. This concentration is within the range used for *in vivo* experiments (Lucidi-Phillipi et al., 1996; Pizzorusso et al., 1999). The REX antibody was a gift from Dr. Louis Reichardt (University of California, San Francisco, San Francisco, CA). Finally, the vehicle control consisted of the administration of sterile saline. NGF treatment started on the day of axotomy (two animals), but administration of NGF+K252a (two animals) or NGF+K252a+REX (two animals) started 15 d after NGF treatment. Three additional animals from our previous study (Davis-López de Carrizosa et al., 2009) that were only axotomized and had received saline injections were also used.

Western blot analysis. Three cats were deeply anesthetized (sodium pentobarbital, 60 mg/kg, i.p.) upon termination of recording experiments to dissect extraocular muscles. This tissue was homogenized in cold lysis buffer containing a mixture of protease and phosphatase inhibitors, disrupted by sonication and centrifuged at 13,000 rpm for 30 min at 4°C. The supernatants were isolated and total protein concentration was determined by the Bradford method (Bradford, 1976), using bovine serum albumin (BSA) as a standard. Proteins were diluted in sample buffer, denatured at 95°C for 6 min, and then separated by 15% SDS PAGE (50 μg/lane). They were then transferred to polyvinylidene difluoride membrane by electroblotting. Nonspecific binding sites were blocked with 5% BSA for 1 h and then the blots were incubated overnight at 4°C in a solution containing an antibody against NGF (1:200, sc-548, Santa Cruz Biotechnology) diluted in TBS-Tween 0.1% supplied with 5% BSA. The membranes were incubated in HRP-conjugated anti-rabbit antibody (1:200) for 1 h at room temperature. The immunoreaction was detected with an ECL Western blotting kit (GE Healthcare). Bands were visualized on Image Reader LAS-3000 (Fujifilm).

Immunocytochemical procedures for fluorescent confocal microscopy. Six animals were prepared just for histology. Two per group received NGF, NGF+REX, or NGF+REX+K252a for 15 d after axotomy. Two additional animals from our previous study were just axotomized (Davis-López de Carrizosa et al., 2009). After terminal anesthesia (sodium pentobarbital, 60 mg/kg, i.p.), animals were perfused intracardially with physiological saline followed by 4% paraformaldehyde in 0.1 M phosphate buffer, pH 7.4. The brain was extracted and postfixed in the same solution for another 2 h. A vibratome was used to obtain 50-μm-thick coronal sections containing the abducens nucleus. These were washed in 0.01 M phosphate buffer, pH 7.4, with 0.9% saline and containing 0.1% Triton X-100 (PBS/TX), and then nonspecific binding sites were blocked with normal donkey serum (10% in PBS/TX) and left overnight at 23°C in different combinations of primary antisera. Triple immunofluorescence labeling was, in general, for choline acetyltransferase (ChAT) for motoneurons, synaptophysin (SYN) for synaptic boutons, and glial fibrillary acidic protein (GFAP) for astrocytes. Dual immunofluorescence was usually performed against ChAT and either TrkA (for NGF high-affinity receptor) or the low-affinity $p75^{NTR}$. Primary antisera cocktails were performed by mixing the following primary antibodies and dilutions: ChAT (goat pAb, 1:300; Millipore), SYN (rabbit pAb, 1:500; Zymed Laboratories), GFAP (mouse mAb G-A-5, 1:800; Sigma), TrkA (directed against a specific peptide mapping adjacent to the carboxy terminus of the TrkA receptor; rabbit pAb, 1:400; Santa Cruz Biotechnology) and $p75^{NTR}$ (rabbit, 1:200; a gift from Dr. Louis Reichardt). VGAT immunoreactivity was used to calculate which fraction of the total number of boutons was inhibitory (González-Forero et al., 2004). VGAT is the vesicular transporter of GABA and glycine (rabbit pAb, 1:500; Millipore). After washing, sections were incubated for 1–1.5 h in a second mixture of antibodies fluorescently tagged as follows: donkey anti-rabbit IgG coupled to Cy2, donkey anti-goat IgG coupled to Cy3 and donkey anti-mouse IgG coupled to Cy5 (Jackson ImmunoResearch). Secondary antibodies were diluted 1:50 to 1:100 in PBS/TX. Finally, sections were washed in PBS and mounted on glass slides and coverslipped with Dako-Cytomation fluorescent mounting medium (Dako).

Confocal microscopy (Leica TCS SP2) at high magnification was used to sequentially capture images at the same focal plane by means of different filters and merged in ImageJ (NIH). Gray scales were adjusted to maximize their dynamic range. Neurons included in the analysis were randomly sampled at high magnification (×63) in 1–4 different focal planes containing the nucleus and separated by 2–3 μm along the *z*-axis. SYN- or VGAT-immunoreactive (IR) boutons were counted to calculate the linear density of boutons. The synaptic coverage was also measured as the percentage ratio between the perimeter occupied by SYN-IR, VGAT-IR terminals, or GFAP-IR profiles over the ChAT-positive somata of motoneurons (Pastor et al., 1997). The $p75^{NTR}$ and TrkA receptor mean gray value was also determined within the somatic boundaries of ChAT-positive motoneurons and scaled to the somatic area. The mean gray value in the neuropil of SYN, VGAT, and GFAP was also measured using square boxes of 30.4 μm per side (80 pixels per side), sampled through the neuropil of images captured at ×40. This measurement was considered an index of the optical density of immunolabeling in the nucleus and was computed as the average gray value within the selection after background level subtraction. That is, the sum of the gray values of all the pixels (8-bit resolution) divided by the number of pixels. For comparisons between groups, one-way ANOVA at a significance level of $p < 0.05$ followed by *post hoc* comparisons were performed in Sigma Plot 11 (Systat Software).

Results

TrkA and $p75^{NTR}$ expression in abducens motoneurons are modulated after axotomy

Abducens motoneurons, identified by ChAT immunoreactivity (Fig. 2*A–F*, insets), expressed constitutively the $p75^{NTR}$ (Fig. 2*A*) and the TrkA receptor (Fig. 2*D*) (Benítez-Temiño et al., 2004) in the form of a speckled immunoreactive pattern covering the cell body and axons (Fig. 2*A*,*D*,*H*). The mean gray value of both NGF receptor immunoreactivities at the somatic level increased 15 d after axotomy (ANOVA; $p < 0.001$) (Fig. 2*B*,*E*,*G*). NGF administration to the cut nerve demonstrated a partial recovery of the $p75^{NTR}$ receptor, although it was still higher than normal values, whereas TrkA immunoreactivity was similar to axotomy and therefore higher than control (Fig. 2*C*,*F*,*G*). NGF receptors have been shown to be upregulated after axotomy (Johnson et al., 1999; Cui et al., 2002; Yuan et al., 2006) and after activation of the TrkA receptor (Rankin et al., 2008). The presence of NGF in the extraocular muscles was demonstrated by Western blot, as illustrated for the lateral rectus (Fig. 2*I*). A dense band at ~15 kDa, corresponding to the mature form of NGF protein, and several

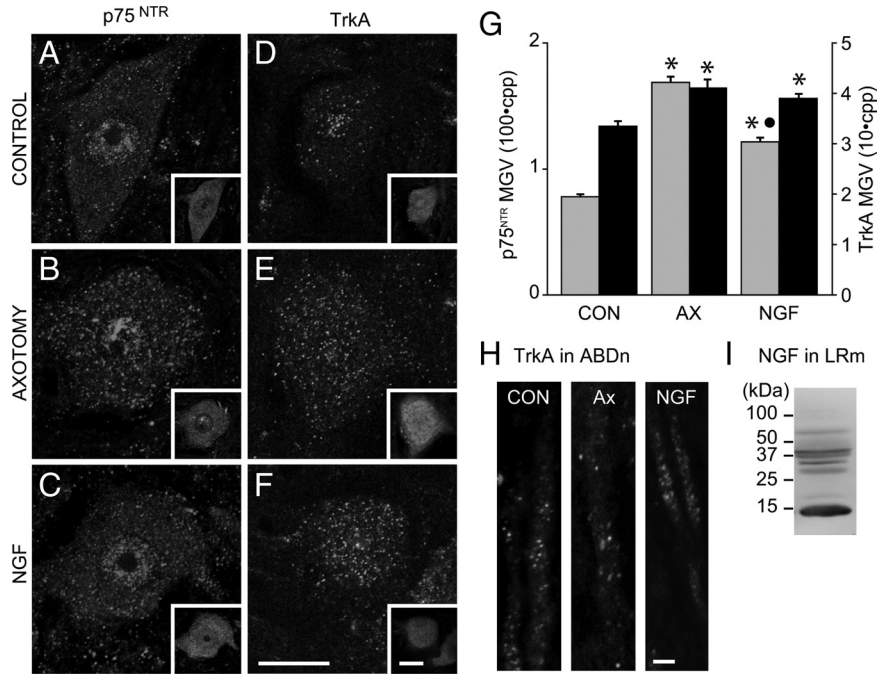

Figure 2. Changes on the expression of p75 ^{NTR} and TrkA. ***A–C***, Motoneurons illustrating p75 ^{NTR} immunostaining in control (***A***), 15 d after axotomy (***B***), and 15 d treated with NGF after axotomy (***C***). Insets show ChAT immunoreactivity for the same motoneurons. ***D–F***, Same as ***A–C***, but for TrkA immunostaining. ***G***, Changes in cytoplasmic mean gray value (MGV in counts per pixel, cpp) after p75 ^{NTR} (gray bars) and TrkA (black bars) immunoreactivity. Asterisks and dots indicate differences with respect to the control and axotomy groups, respectively (ANOVA, Holm-Sidak method for pairwise multiple comparisons, $p < 0.01$). ***H***, Axons in the rootlets of the abducens nerve (ABDn) demonstrating TrkA immunoreactivity. ***I***, Immunoblotting showing the expression of NGF protein in the lateral rectus muscle (LRm). Size markers units are kDa. CON, Control; Ax, axotomy. Scale bars: ***F***, 20 μm; ***H***, 2 μm.

bands at ~32 and 40 kDa, indicative of NGF precursors (Buttigieg et al., 2007), were observed.

NGF reinstates the firing pattern of axotomized abducens motoneurons

The tonic and phasic firing of abducens motoneurons during spontaneous eye movements has been extensively described (Delgado-García et al., 1986). Control abducens neurons had a tonic and regular discharge for eye position during eye fixations (Fig. 3*A*) that increased proportionally to the degree of eye rotation directed toward the ipsilateral side of recording, namely the on-direction, represented by a leftward movement recorded in a motoneuron on the left side (Figs. 3*A*, 4*A*, numbers depicted 1 through 4). Firing decreased proportionally, and eventually stopped whenever the eye moved toward the off-direction (Figs. 3*A*, 4*A*, numbers indicated 5 through 7). The correlation of firing rate versus eye position allowed calculation of the eye position sensitivity (Fig. 4*B*). The slope of the linear regression line obtained between the firing rate and the eye position represents the neuronal sensitivity to eye position (k, measured in sp/s/deg) (Fig. 4*B*). The mean eye position sensitivity computed from 70 control abducens motoneurons was 6.4 ± 0.26 sp/s/deg (Table 1). The abscissa intercept of the firing rate to eye position plot is considered the eye position at which the unit is recruited into activity (Fig. 4*B*). Mean recruitment threshold was $-7.1 \pm 0.86°$ in control motoneurons (Table 1). Motoneuronal activity was also related to eye velocity during saccades, thus motoneurons displayed high-frequency bursts and pauses during on- and off-directed saccades, respectively (Fig. 4*A*, red box). The slope of the linear regression analysis between firing rate and eye velocity was the sensitivity to eye velocity, namely r (Fig. 4*C*). In control motoneurons, $r = 0.73 \pm 0.04$ sp/s/deg/s (Table 1).

The firing pattern of abducens motoneurons (Fig. 3*B*), but not that of internuclear neurons (data not shown), was perturbed after VIth nerve axotomy (Delgado-García et al., 1988; Davis-López de Carrizosa et at., 2009). Changes took place over the first week and did not recover during the entire survival time (Fig. 4*D*, green circles). Axotomized motoneurons showed an overall reduction in firing rate and a severe decay of modulation related to eye position and velocity (Fig. 3*B*, Table 1). By contrast, administration of NGF immediately after lesion not only prevented the decay in eye position and velocity sensitivities due to axotomy, but also quickly restored the firing pattern of motoneurons and enhanced their sensitivities to the parameters of eye movement (Fig. 3*C*,*D*). However, the effects of retrograde administration of NGF through the cut nerve produced other changes in the firing pattern that were apparent from the first week after treatment (around the second recording session) (Fig. 4*D*, blue triangles). NGF produced a significant rise in both eye position (9.37 ± 0.30 sp/s/deg) and velocity (0.93 ± 0.03 sp/s/deg/s) sensitivities with respect to control (Table 1, Fig. 4*D*, gray band labeled as NGF) ($p < 0.05$). These were maintained at high levels throughout the course of the experiment (Figs. 3*C*,*D*, 4*D*, blue triangles). Remarkably, motoneuronal recruitment threshold was shifted toward more eccentric eye positions (Table 1). We believe this may be indicative of higher levels of inhibition, despite the overall higher sensitivities to eye position and velocity compared with control. Results on motoneuronal recruitment threshold will be presented later.

A concerted action of NGF through TrkA and p75 ^{NTR} receptors

We tested whether the effects of NGF on abducens motoneurons were mediated via high- and/or low-affinity receptors by the sequential blocking of TrkA and p75 ^{NTR} by using K252a and REX, respectively, as selective inhibitors. Because axotomized motoneurons first showed significant differences from control cells after 14 d (Fig. 4*D*, green circle at 14 d) ($p < 0.05$), we initiated the pharmacological blockade of NGF receptors by this time. We administered NGF+K252a 15 d after the axotomized motoneurons had been treated with NGF (Fig. 3*E*). K252a added to NGF did not alter the motoneuronal firing modulation with eye position and eye velocity compared with control (Fig. 3*E*). Motoneuronal sensitivity decayed rapidly, and within ~5 d it stabilized at values that were different from the axotomy and the NGF paradigm (Fig. 4*D*, cyan squares), but not different from control values (Table 1). This result indicated that NGF acting through the p75 ^{NTR} alone was sufficient to restore the firing sensitivity of the motoneuron, but when p75 ^{NTR} acted together with the TrkA receptor, the effects were cooperative, resulting in sensitivities that rose above control. Moreover, the dual blockade of both

types of NGF receptor with K252a and REX led to the complete blockade of NGF actions (Fig. 3*F*). In this case, the overall firing rate of motoneurons resembled the behavior after axotomy, showing very low sensitivities (Fig. 4*D*, red diamonds) that were similar to the axotomy values (Table 1). It should be noted that, in contrast with axotomy, motoneurons that were doubly blocked fired in a continuous, low-modulation mode, as if they were disinhibited, but with very little excitatory drive (Fig. 3*F*). These results suggest that the sensitivities of axotomized motoneurons were enhanced by one receptor to control values and further boosted when both receptors were activated by NGF.

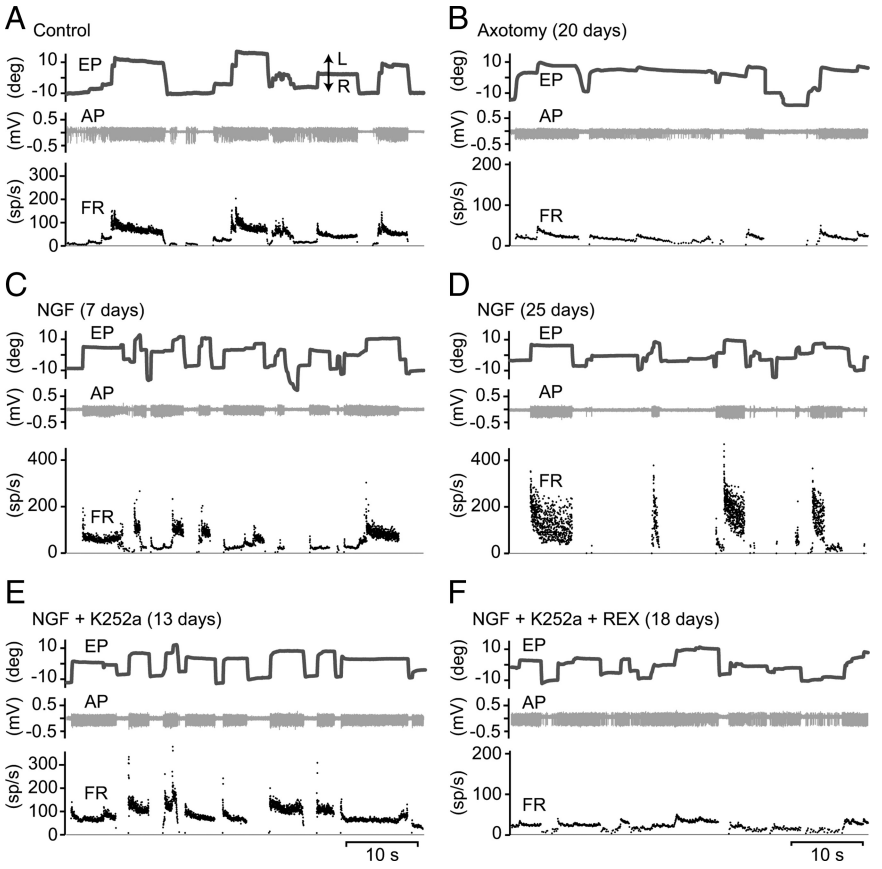

Figure 3. Effects of NGF and NGF receptor blockers on the discharge pattern of abducens motoneurons. ***A***, Firing rate (FR) profile of a control abducens motoneuron recorded during spontaneous eye movements. The single-unit discharge of action potentials (AP) is shown in the middle trace. EP, Eye position; L, movement to the left; R, movement to the right. ***B***, Same as ***A***, but for a motoneuron recorded 20 d after axotomy without reinnervation. Note reduced firing during both saccades and spontaneous fixations. ***C***, ***D***, NGF treatment causes recovery of the burst-tonic firing pattern; however, the discharge variability increased during eye fixations. ***E***, Motoneurons treated with K252a still showed part of the effects produced by NGF, indicating that part of the effects of NGF could also be mediated via the p75 ^{NTR}. ***F***, Motoneurons treated with K252a and the p75 ^{NTR} blocker REX demonstrated an axotomy-like firing profile although they were firing continuously.

Recruitment threshold changes with activation of p75 ^{NTR}

Recruitment threshold, calculated as the abscissa intercept of the rate-position plot, changed after NGF treatment (supplemental Fig. 1*A*, available at www.jneurosci.org as supplemental material). Abducens motoneurons show orderly recruitment patterns that correlate with neuronal sensitivity (Pastor and González-Forero, 2003). Thus, when regression lines between firing rate and eye position are plotted for individual cells, the slopes (k) are higher as the cells become recruited further toward ipsilateral eye positions (supplemental Fig. 1*B*, available at www.jneurosci.org as supplemental material, for the 70 control motoneurons recorded). When we plotted eye position sensitivity (k) versus recruitment threshold for each neuron, an exponential correlation was found for each experimental group (supplemental Fig. 1*C*,*D*, available at www.jneurosci.org as supplemental material). Motoneurons treated with NGF not only had higher sensitivities to eye movements—that is, both the tonic sensitivity (k) during fixations and the phasic sensitivity (r) during saccades were enhanced—but they also showed a higher recruitment threshold (Table 1). The recruitment threshold, i.e., the eye position at which the motoneuron first enters into activity, shifted from a mean of ~ -6 to $-7°$ in control and axotomized motoneurons to $\sim -2°$ in NGF-treated cells (Table 1; supplemental Fig. 1*A*, available at www.jneurosci.org as supplemental material). Interestingly, NGF+K252a-treated cells (block of the high affinity receptor) did not show this modification of the average recruitment threshold, indicating that the shift in recruitment threshold was due to p75 ^{NTR}. Furthermore, when we blocked both types of NGF receptor, the recruitment threshold returned to axotomized (similar to control) values (Table 1, supplemental Fig. 1*A*, available at www.jneurosci.org as supplemental material).

Alterations in firing variability are due to p75 ^{NTR} activation

It was noticed that the variability of firing changed in response to the treatments. This was best seen in instantaneous firing frequency traces, which showed larger variability compared with controls (Figs. 3, 5*A–C*). To analyze firing regularity, we selected periods with stationary firing rate (Fig. 5*D–F*). The histograms of the interspike intervals (ISI) were constructed with at least 80 intervals from the same eye fixation (Fig. 5*G–I*). ISI histograms followed normal distributions (Kolmogorov–Smirnov test, $p > 0.05$), except those from NGF-treated cells, which displayed Poisson-like distributions that were highly skewed toward long intervals. Control cells had the smallest variance of ISIs (Fig. 5*G*). In contrast, NGF-treated motoneurons showed a distribution with both shorter and longer intervals (Fig. 5*I*). The values of axotomized neurons were slightly expanded toward longer intervals (Fig. 5*H*). Autocorrelation histograms showed that control motoneurons produced highly regular spike trains. In control and axotomized motoneurons, up to eight peaks were readily observed in the autocorrelogram (Fig. 5*J*,*K*). However, no repetitive pattern could be seen in the autocorrelograms of NGF-treated cells (Fig. 5*L*).

The dependence of the SD of the mean firing rate on the mean firing frequency has been previously described in spinal and extraocular motoneurons (Powers and Binder, 2000; González-Forero et al., 2002). We selected the coefficient of variation (i.e., the percentage ratio of the SD to the mean), because it is insensitive to scale changes and thus adequate to establish comparisons between groups. The coefficient of variation was higher at lower frequencies but decreased at higher frequencies, as exemplified

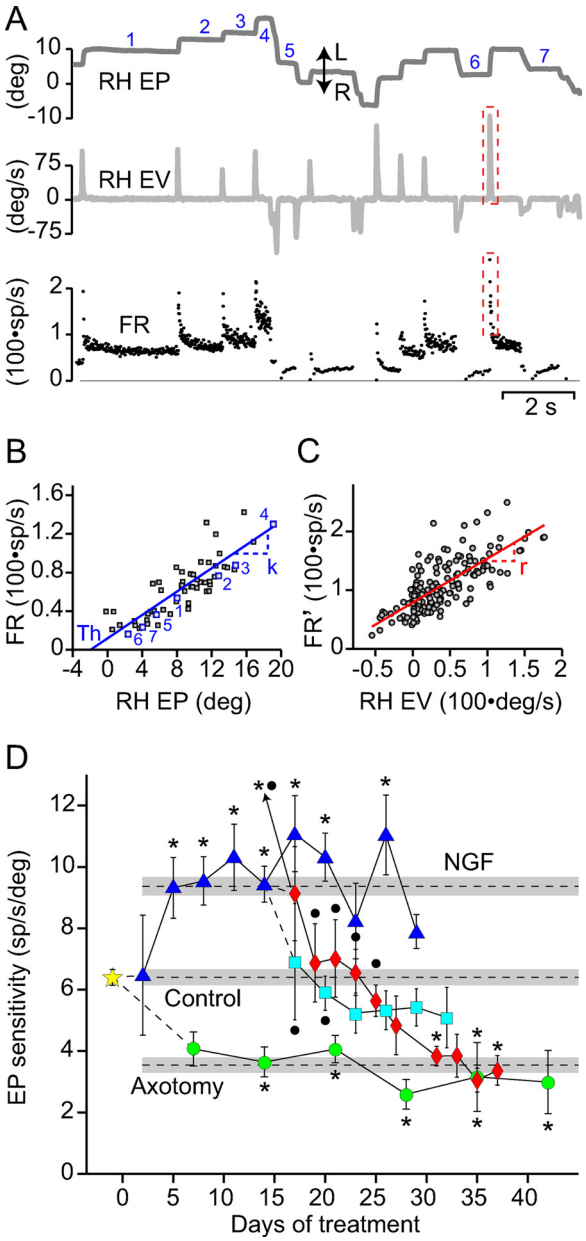

Figure 4. NGF produces recovery of the discharge characteristics of axotomized motoneurons. ***A***, Control motoneurons burst for on-directed saccades and fire tonically during eye fixations. Panels show from top to bottom: right horizontal eye position (RH EP), velocity (RH EV), and the firing rate (FR). L, Movement to the left; R, movement to the right. ***B***, Regression plot of the motoneuron shown in ***A*** obtained during spontaneous fixations. Some of the fixations are labeled with numbers both in ***A*** and ***B***. The slope of the regression line is the eye position sensitivity of the motoneuron (k). In this case, $k = 7.0$ sp/s/deg ($r = 0.89$; $p < 0.001$). The intercept with the abscissa represents the eye position for neuronal recruitment. Th, Threshold. ***C***, Partial regression plot during spontaneous saccades (like the boxed area in red in ***A***) obtained after plotting firing rate, minus the position component, versus eye velocity. The slope of the regression line is the eye velocity sensitivity of the motoneuron (r). In this case, $r = 0.75$ sp/s/deg/s ($r = 0.74$; $p < 0.001$). ***D***, Time course of changes in eye position sensitivity of motoneurons that received the different treatments. The yellow star indicates the control population mean. NGF-treated cells are indicated with blue triangles and axotomized ones with green circles. The dual NGF-receptor blocking treatments started 15 d after NGF treatment and consisted on NGF + K252a (cyan squares) and NGF + K252a + REX (red diamonds). The dashed lines and gray bands indicate the mean and SE of the control, axotomized, and NGF-treated populations. Asterisks and dots indicate differences with the control and axotomy group, respectively (ANOVA; Holm-Sidak; $p < 0.05$).

for 2097 periods obtained from 70 control motoneurons. The coefficient of variation versus firing rate was fitted by a double exponential function (Fig. 6*A*). The firing variability was slightly higher than the control in the axotomized motoneurons, but extraordinarily larger in those treated with NGF at all frequencies tested (ANOVA, $p < 0.05$) (Fig. 6*B*). We compared the variability across groups in the frequency range where the coefficient of variation was relatively stable and motoneurons of all groups were represented, that is, between 30 and 80 sp/s (Fig. 6*C*). Firing variability was slightly higher than the control in the axotomy group, much larger in the NGF group, and slightly less when the TrkA receptor was blocked, with all these differences being significant ($p < 0.05$). The variability returned to axotomy level only when both NGF receptors were blocked (ANOVA, Holm-Sidak, $p < 0.05$) (Fig. 6*C*, red bar). Therefore, firing variability was mainly controlled through the activation of $p75^{NTR}$.

NGF synaptotrophism prevents synaptic stripping

Functional alterations, as described above, could arise because of changes in the synaptic composition of inputs to the motoneuron. The somatic surface coverage of synaptic and glial processes was measured by means of immunoreactivity against SYN and GFAP, respectively. To determine the ratio of inhibition to excitation, we measured the synaptic coverage of inhibitory boutons by using immunostaining against VGAT. In control abducens motoneurons, 46.1 ± 2.0% of the somatic perimeter was surrounded by SYN-IR boutons (Figs. 7*A* and 8) and only 8.7 ± 1.4% was covered by astroglial filaments (supplemental Fig. 2*A*, available at www.jneurosci.org as supplemental material). Approximately 70% of the somatic boutons were VGAT-IR in controls (Fig. 7*B*). Axotomy reduced the coverage of SYN-IR boutons to 21.4 ± 2.1% (ANOVA, $p < 0.05$) (Fig. 8); a large proportion of the remaining boutons were VGAT-positive. In contrast, astrocyte processes proliferated to cover up to 40.1 ± 1.6% of the cell surface (supplemental Fig. 2, available at www.jneurosci.org as supplemental material, Axotomy). The administration of NGF to axotomized motoneurons prevented the drop in both SYN-IR and VGAT-IR boutons (Figs. 7 and 8, NGF). NGF also reduced the GFAP reaction induced by axotomy to an intermediate level (14.1 ± 1.1%) (supplemental Fig. 2, available at www.jneurosci.org as supplemental material, NGF). Blockade of NGF action via $p75^{NTR}$ with the REX antibody also prevented SYN-IR synaptic stripping (Fig. 8, NGF+REX), indicating that the synaptotrophic action of NGF occurred through the TrkA receptor. Finally, the dual blockade of NGF receptors produced an axotomy-like elimination of boutons (Fig. 8, NGF+K252a+REX). Changes in the density of SYN-IR and VGAT-IR boutons occurred in parallel in the different experimental groups except for the NGF+REX treatment (Fig. 8). The neuropil of the abducens nucleus showed similar quantitative changes as in the perimeter of motoneurons. Mean gray value, an index of the optical density, measured in the neuropil, demonstrated a similar trend in synaptic coverage with SYN-IR and VGAT-IR profiles (Fig. 7,*C*,*D*, supplemental Fig. 2*B*, available at www.jneurosci.org as supplemental material).

Remarkably, the ratio of VGAT-IR to SYN-IR boutons changed from 0.75 in control to 0.6 in the doubly blocked NGF-treated motoneurons, indicating a reduction in the proportion of inhibitory boutons. However, the ratio with respect to control did not change in axotomy, NGF-treated, or NGF+REX groups (χ^2 test, $p > 0.05$). The fact that the ratio of inhibition to excitation was larger in the control and NGF-treated cells than in double-blockade cells was in agreement with the physiological

Table 1. Effects of NGF and receptor blocking on motoneuronal sensitivities and recruitment threshold

Treatment	*N*	*k* (sp/s/deg)	*r* (sp/s/deg/s)	Th (deg)
Control	70	6.40 ± 0.26	0.73 ± 0.04	−7.10 ± 0.86
Axotomy	53	3.54 ± 0.25*	0.47 ± 0.03*	−6.62 ± 1.00
NGF	134	9.37 ± 0.30*†	0.93 ± 0.03*†	−2.22 ± 0.31*†
NGF+k252a	46	5.31 ± 0.34†‡	0.65 ± 0.04†‡	−1.59 ± 1.51*†
NGF+k252a+REX	39	4.34 ± 0.27*‡	0.53 ± 0.04*‡	−5.28 ± 0.73

Values are means ± SEM. Symbols indicate significant differences between control (*), axotomy (†), and NGF (‡) groups (one-way ANOVA, Holm–Sidak method for *post hoc* comparisons, $p < 0.05$). Th, Threshold.

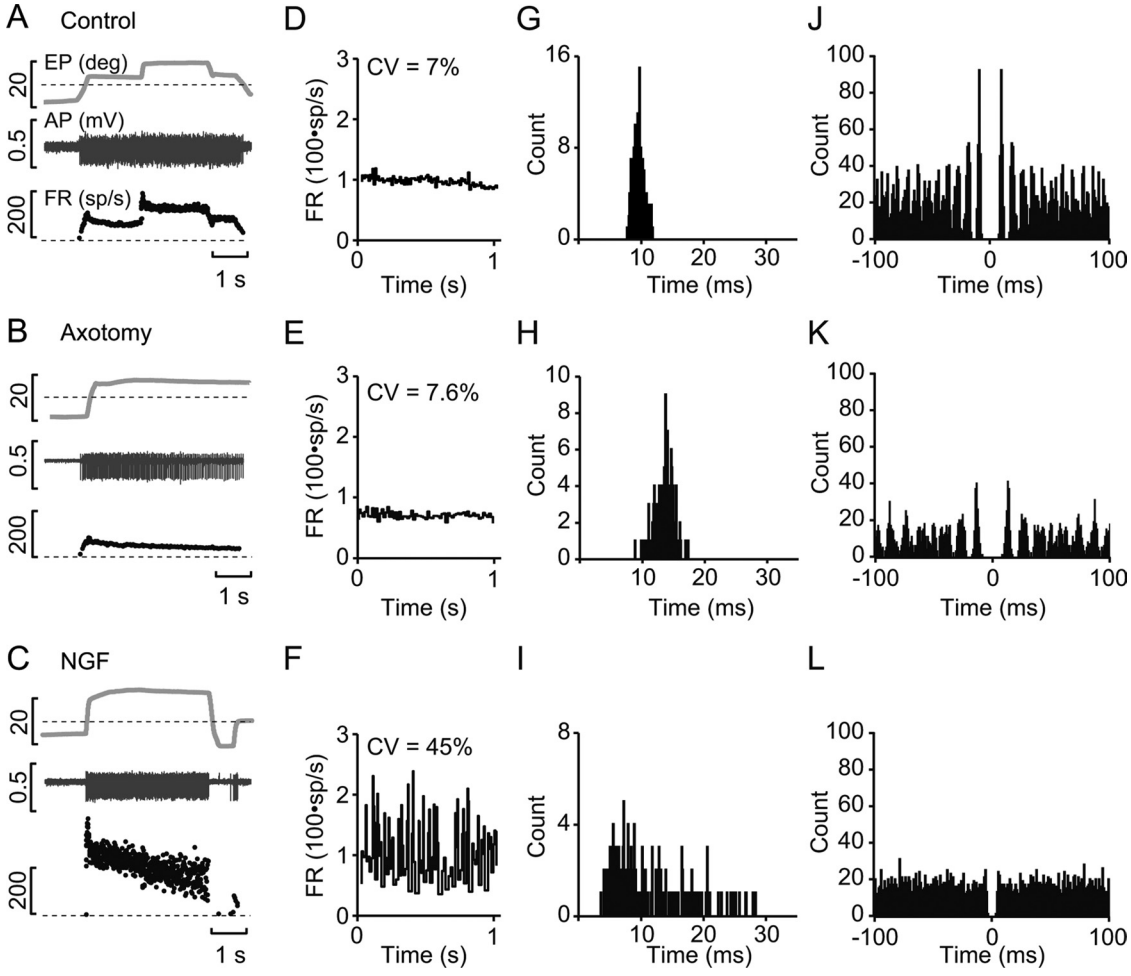

Figure 5. NGF effects on the discharge variability of axotomized motoneurons. ***A–C***, Firing patterns of control (***A***), axotomized (***B***), and axotomized but NGF-treated (***C***) motoneurons. The firing rate (FR) in control and axotomized motoneurons showed a highly regular profile during spontaneous eye movements (EP). The single-unit discharge of action potentials (AP) is shown in the middle trace. ***D–F***, Periods of 1 s of instantaneous firing rate in a control (***D***), axotomized (***E***), and NGF-treated (***F***) abducens motoneuron. Stationary periods were selected as having similar mean firing rate across groups. Note, however, the large increase of both the SD and the coefficient of variation (CV) in ***F***. ***G–I***, First-order ISI histograms from the corresponding cells shown in ***A–C***, but constructed using a 2 s sample (bins of 0.1 ms). Distributions were normal except in ***I*** (Kolmogorov–Smirnov test; $p > 0.05$), which showed a high skew to the right. ***J***, The control autocorrelogram (1 ms bin size) showed one clear peak, isolated from the base, and up to three clear peaks, fused in the base (same cell as in ***A***, ***D***, and ***G***). ***K***, The autocorrelogram of the axotomized motoneuron shown in ***B*** and ***E*** demonstrated a somewhat higher variability than the control motoneuron. ***L***, The autocorrelogram of the NGF-treated motoneuron illustrated in ***C*** and ***F*** showed a complete absence of spike predictability.

recordings. These motoneurons showed much higher levels of inhibition in overall firing than after NGF treatment. In contrast, inhibition was scarce after double blockade (Fig. 3, notice the large periods of inhibition in *C* and *D* vs the almost continuous low-rate discharge in *F*). Thus, it appears that if NGF-treated cells showed a larger excitation, they also must have an equally large inhibition, whereas the contrary can be applied for the double-blockade group (i.e., the more reduced the excitation, the less inhibition was present).

Changes in the inhibition to excitation balance

To check this idea, we measured *k*-on and *k*-off as an index of the excitation and the inhibition received by the motoneurons during firing activity. The *k*-on value was measured as the slope of the regression line between firing rate and fixations attained after on-directed saccades. The opposite held for the *k*-off parameter. Axotomy reduced both the *k*-on and *k*-off values and NGF treatment elevated both above the control level (ANOVA test, $p < 0.05$) (Fig. 9*A*). The progressive blockade of NGF receptors demon-

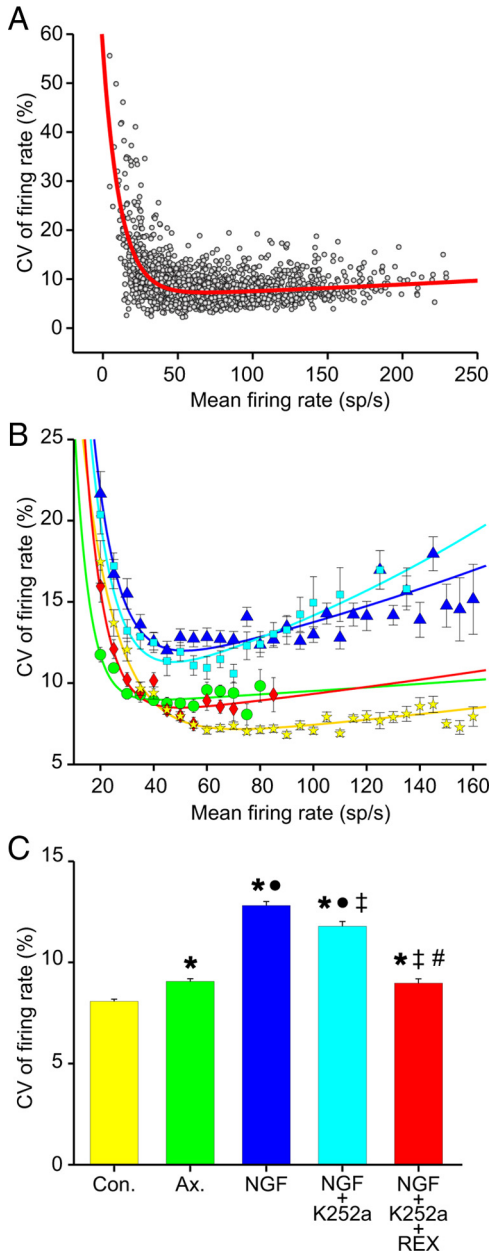

Figure 6. Blockade of NGF receptors restores firing variability of axotomized motoneurons. ***A***, Plot of the coefficient of variation (CV) versus the mean firing frequency of 2097 stationary periods obtained from 70 control motoneurons. Note that higher CV accompanies lower firing frequencies. ***B***, Firing variability (CV) of all experimental groups showed an exponential decay as the discharge rate increased (color codes as shown in ***C***). Fitted lines are double exponentials with $R^2 > 0.95$ in all cases ($p < 0.001$). Values are represented as mean ± SEM of CV in percentage of different firing frequencies spaced every 5 Hz. All comparisons between groups were significantly different (ANOVA test, Tukey test for *post hoc* comparisons, $p < 0.001$). ***C***, Comparison of CV in the interval 30 – 80 sp/s. Note that NGF treatment dramatically increased the firing variability, whereas blockade of TrkA receptors partially decreased variability, and blockade of both p75 ^{NTR} and TrkA receptors restored firing variability to axotomy levels (ANOVA test, Holm–Sidak method, $p < 0.05$). Symbols indicate significant differences between control (*; Con.), axotomy (●; Ax.), and NGF treatment (‡) experimental groups. #, NGF+K252a treatment.

strated that both parameters decayed partly with the K252a treatment and totally when the dual block of NGF receptors was used, resulting in values similar to axotomy (Fig. 9*A*). The overall consequences of NGF treatment and blockade are summarized in Figure 9*B*. The overall effect of NGF treatment is a counterclockwise rotation of the regression line computed as higher slope (Fig. 9*B*, blue line). Conversely, the overall effect of the NGF dual blockade is a clockwise rotation (lower slope) of the line (Fig. 9*B*, red line) to values similar to the axotomy state. However, in this case, the ratio of inhibition to excitation was smaller than what was expected from a simple clockwise rotation of the control group (compare the different angles between the solid and dashed red lines and the corresponding solid and dashed blue lines in the lower left quadrant of Fig. 9*B*). Thus, motoneurons with less activity, i.e., the group treated with NGF+K252a+REX, also showed proportionally less inhibition.

Discussion

Our results show that NGF is a trophic factor for adult abducens motoneurons that restores afferent innervation and discharge characteristics after axotomy. NGF treatment resulted in the prevention of the lesion-induced stripping of synaptic boutons and reestablished the excitability and neuronal sensitivities to eye movements by acting through both p75 ^{NTR} and TrkA receptors. This is the first *in vivo* evidence that complementary retrograde signaling through the two different NGF receptors results in the regulation of firing patterns through changes in the excitability and composition of input to motoneurons.

Effects of NGF on synaptic coverage

Treatment with NGF did not induce synaptic stripping of motoneuron membranes caused by axotomy on motoneurons. This effect was mainly due to the action of NGF via TrkA, since blocking p75 ^{NTR} did not induce synaptic stripping in axotomized animals treated with NGF, and only when both NGF receptors were blocked did synaptic loss occur. It is well known that axotomy induces considerable synaptic stripping, and that the degree of deafferentation depends on manipulations of target reinnervation (Sumner, 1975). Thus, if neurons reinnervate any target, the effects of axotomy wane (Delgado-García et al., 1988; Brännström and Kellerth, 1999), but neurons remain partly deafferented when target reinnervation is prevented (Pinter and Vanden Noven, 1989). Our NGF treatment results in a high responsiveness of axotomized motoneurons to this neurotrophin. Both the phasic and tonic firing increased, and only after the complete blockade of NGF receptors did the sensitivities return to axotomized levels. Phasic firing during saccades is provided by excitatory and inhibitory reticular neurons located in the paramedian pontomedullary reticular formation (Büttner and Büttner-Ennever, 2006). The tonic component arises from the output of a velocity-to-position integrator connected to motoneurons (Aksay et al., 2001). It is likely that NGF exerts a trophic effect through synaptic contacts by these inputs to the abducens motoneurons. In fact, NGF is known to have a robust synaptotrophic role, regulating aspects of synaptic transmission such as synaptophysin expression, neurotransmitter release, expression of synaptic receptors, and changes in synaptic efficacy (Mendell and Arvanian, 2002; Cotrufo et al., 2003; Hazary et al., 2007; Huh et al., 2008; Tarsa and Balkowiec, 2009).

Expression of p75 ^{NTR} and TrkA receptors

Unlike other cranial and spinal motoneurons (Lindsay, 1994; Ferri et al., 2002), extraocular motoneurons are peculiar in that they express TrkA receptors (Benítez-Temiño et al., 2004). Therefore, the modulation and expression of both p75 ^{NTR} and TrkA receptors in the presence or absence of NGF was also distinct. There is variability in the occurrence of the Trk receptors, such that cranial and spinal motoneurons do contain Trk recep-

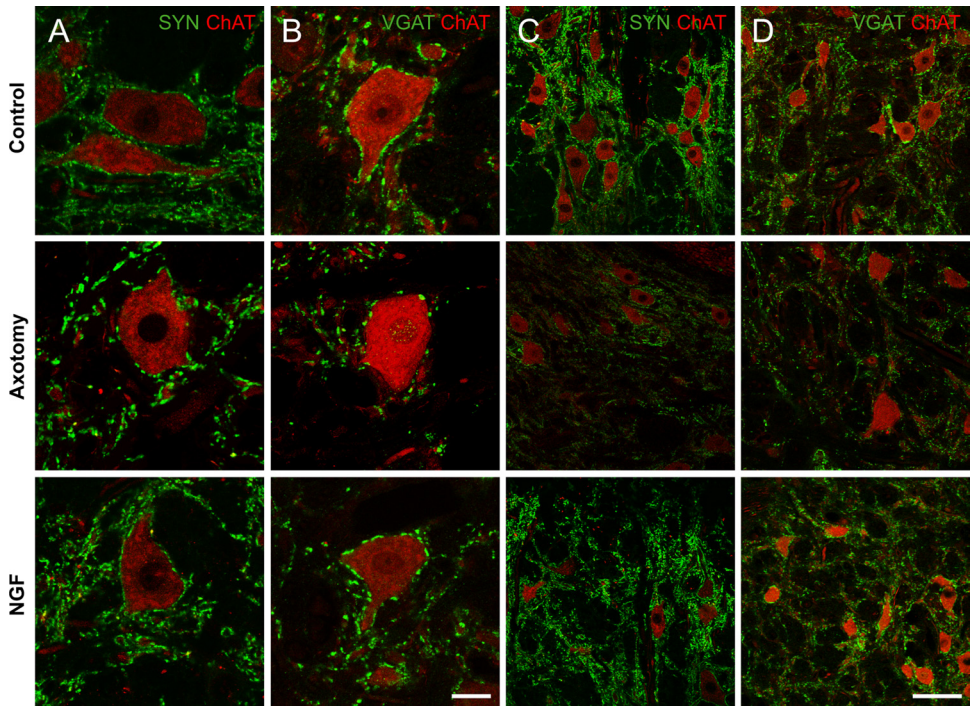

Figure 7. NGF prevents synaptic stripping of motoneurons. ***A–D***, Confocal images of motoneurons in control, axotomy, and NGF-treated groups illustrating the innervation (green; ***A***, ***C***) or the inhibitory boutons labeled with antibody against VGAT (green; ***B***, ***D***), or the ChAT-labeled motoneuronal cell bodies (red; ***A–D***). All sections were obtained from animals 15 d after either axotomy or axotomy and treatment. Note the marked reduction of boutons after 15 d of axotomy. Scale bars: ***B***, 20 μm; ***D***, 80 μm.

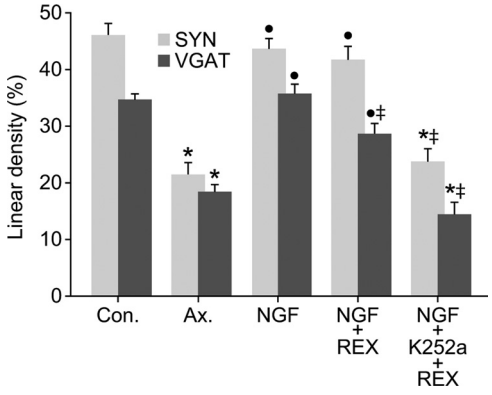

Figure 8. NGF promotes maintenance of afferent innervation on motoneurons. The linear density of synaptophysin-IR (SYN) and VGAT-IR (VGAT) boutons over the somatic perimeter of motoneurons changes after axotomy and the different treatments. Bars represent mean ± SEM for 17–38 motoneuronal profiles in each group. Symbols indicate differences between control (*; Con.), axotomy (●; Ax.), and NGF (‡) groups. ANOVA, Holm–Sidak method for multiple pairwise comparisons ($p < 0.05$).

tors, but only TrkB and TrkC are present in adults (Merlio et al., 1992; Henderson et al., 1993; Koliatsos et al., 1993; Piehl et al., 1994). During development, spinal motoneurons contain TrkA receptors, but their expression is downregulated afterward (Ernfors et al., 1989). Motoneurons affected by ALS shift their expression of Trk receptors from TrkB and TrkC to TrkA (Nishio et al., 1998). In the adult, the expression of TrkA receptors is reinduced by axotomy in retinal ganglion cells (Cui et al., 2002) and in motoneurons (Omura et al., 2005), and lost again after the reinnervation of the target muscle (Koliatsos et al., 1993). NGF has also been shown to affect axotomy responses via the $p75^{NTR}$ (Ferri et al., 2002), which, as in the present data, increases after lesion (Johnson et al., 1999; Yuan et al., 2006). The presence of NGF signaling in abducens neurons might confer greater resistance to the effects of lesions and neurodegenerative diseases (Benítez-Temiño et al., 2004).

Complementary effects via $p75^{NTR}$ and TrkA receptors

It is noteworthy that motoneuronal sensitivities after NGF treatment become higher compared with control. NGF (Hazari et al., 2007), like BDNF and NT-3, also enhances synaptic transmission (Munson et al., 1997; Sherwood and Lo, 1999; Arvanian et al., 2003, Davis-López de Carrizosa et al., 2009). Our data indicates that the maintenance of synaptic coverage (i.e., the lack of synaptic stripping) was dependent exclusively on TrkA receptors. NGF increases in nicotinic transmission that are dependent on TrkA receptor activation have also been demonstrated in parasympathetic motoneurons (Hazari et al., 2007). Moreover, NGF acting through TrkA receptors has been shown to enhance the firing activity over control values in other central cholinergic neurons (Wu and Yeh, 2005). However, the neuronal sensitivities were partly dependent on both NGF receptors, because the blockade of TrkA receptors decreased sensitivities from the high values of the NGF treatment and the dual receptor blockade produced a further decay to axotomy levels.

NGF treatment led to an increase in the ratio of inhibition to excitation, even if TrkA receptor was blocked. These cells showed ample inhibition, as demonstrated by higher recruitment thresholds and longer firing pauses during fixation. In parallel with these response changes, the ratio of VGAT to synaptophysin increased with respect to the dual blockade of NGF receptors, although it did not differ from control ratios. NGF-treated cells also demonstrated more excitation, as shown by larger k values. These larger synaptic drives might be made possible by greater synaptic efficacy, since there was no vacant synaptic space (Huh et al., 2008). Changes in the amount of inhibition appeared to compensate for changes in the excitatory drive in a homeostatic

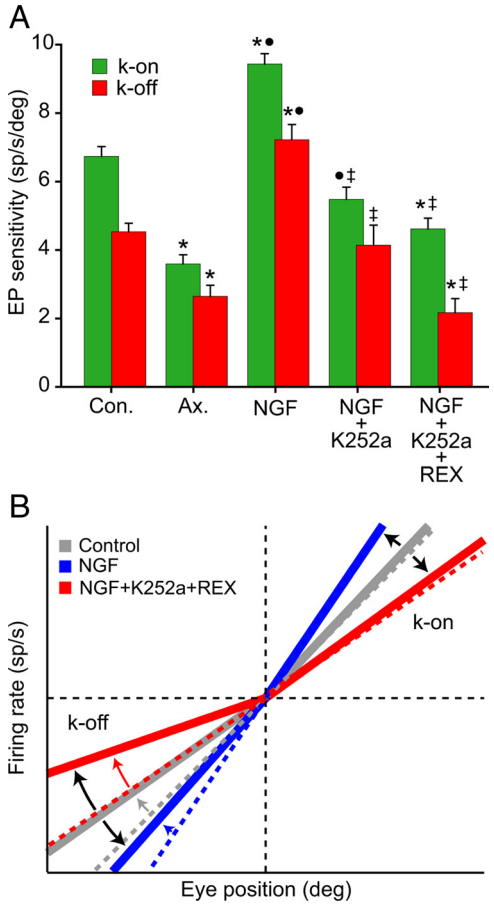

Figure 9. NGF maintains the inhibition to excitation balance. ***A***, Changes in eye position (EP) sensitivity calculated as *k*-on or *k*-off, depending on the direction of the preceding saccade. Note that axotomy decayed both sensitivities, whereas NGF greatly improved them, maintaining the relative proportion of inhibition to excitation. Blocking TrkA receptors reduced sensitivities significantly. However, only *k*-off was further reduced upon the double block (ANOVA, Holm–Sidak method for multiple pairwise comparisons, $p < 0.05$). Symbols indicate differences with control (*; Con.), axotomy (●; Ax.), and NGF (‡) groups. ***B***, Diagram illustrating the sensitivity (*k*; dashed lines) in control (gray), after NGF (blue), and after double NGF receptor blockade (red). Solid lines in the upper-right quadrant indicate the *k*-on values and solid lines in the lower-left quadrant depict the *k*-off sensitivities. The straight gray dashed line indicates the rate-to-position plot of the average control motoneurons. Note that double blockade of NGF receptors reduced the *k*-off (curved red arrow), indicating that motoneurons were markedly disinhibited. To the contrary, the *k*-off and *k*-on values were comparable in both control and NGF-treated cells, despite a trend toward higher inhibition in NGF-treated motoneurons.

fashion, so the larger the excitation during NGF treatment, the larger the inhibition (Palop et al., 2007). The opposite rule applied when the excitatory drive was low during the dual blockade of NGF receptors (Nelson and Turrigiano, 2008).

Changes in the motoneuronal excitability

Motoneurons treated with NGF demonstrated higher recruitment thresholds and discharge variability. Blockade of the TrkA receptor partially reduced firing variability, but the subsequent blockade of $p75^{NTR}$ changed threshold and variability to axotomy values. Recruitment threshold is an index of the excitability and activity of the abducens neurons. This overall activity depends, in part, on the ratio of inhibition to excitation that motoneurons receive. Thus, if this ratio is altered, there are basal activity changes. This was demonstrated with tetanus toxin effects on these motoneurons (González-Forero et al., 2002, 2004). Low doses of tetanus toxin produced disinhibition and, therefore, a low inhibition-to-excitation ratio that decreased recruitment threshold. A similar scenario occurred in our cells treated with NGF+K252a+REX, which produced a disinhibited firing accompanied by lower thresholds than those seen in the motoneurons treated with NGF. Since blockade of TrkA alone did not reduce the recruitment threshold in comparison with the NGF treatment, $p75^{NTR}$ was presumably responsible for disinhibited firing. These results in the double blockade group were also accompanied by lower *k*-off values and lower VGAT coverage than expected. In line with our results, NGF acting through $p75^{NTR}$ has been shown to increase the ratio of inhibition to excitation (Salama-Cohen et al., 2006).

Motoneurons treated with NGF demonstrated a high variability of firing even if TrkA receptors were blocked. NGF has been shown to regulate excitability through several ionic currents (Zhang and Nicol, 2004; Luther and Birren, 2009). One of them is the M-current, likely present in oculomotor motoneurons, as seen with carbachol-induced depolarizations (Nieto-Gonzalez et al., 2009). This current is modulated via the two NGF receptors. Specifically, TrkA activation leads to a reduction of M-current that changes firing from phasic to tonic (Luther and Birren, 2009). NGF has also been also shown to neuromodulate pain sensitization (Shu and Mendell, 1999), due to changes of expression and kinematics of persistent sodium currents and voltage-dependent potassium currents through the $p75^{NTR}$ (Zhang et al., 2002; Zhang and Nicol, 2004). However, it should be noted that any depolarization bringing membrane potential near the spike threshold also contributes to irregular firing due to fluctuations produced by synaptic noise (Calvin and Stevens, 1968), the strategic location of inhibitory inputs near the axon hillock (Shadlen and Newsome, 1998), and the synchronization of inputs (Lampl et al., 1999). Further study is needed to define which of these mechanisms is at work in abducens motoneurons.

A trophic classification of abducens motoneurons?

The present findings extend our analysis of target-dependent neurotrophic responses in abducens motoneurons by showing that the expression of normal morphological and physiological properties are regulated via the retrograde transport of different neurotrophins. We have demonstrated that BDNF leads to tonic firing in motoneurons via TrkB receptors, whereas NT-3 leads to phasic firing through TrkC receptors (Davis-López de Carrizosa et al., 2009). Abducens motoneurons vary with respect to the number of each receptor type with which they are endowed (Benítez-Temiño et al., 2004). Thus, different classes of motoneurons may be defined with respect to their responses to the mixture of trophic factors that are present (Büttner and Büttner-Ennever, 2006). Retrograde regulation may change the gradient of firing patterns, from tonic to phasic, as recently described for sympathetic neurons (Luther and Birren, 2009). Trophic support changes could even explain phenotypic changes observed in ALS spinal motoneurons (Nishio et al., 1998). Thus, the etiology of diseases such as in diabetic neuropathy (Andreassen et al., 2009), cardiac arrests (Ieda and Fukuda, 2009), or Parkinson's disease (Ramaswamy et al., 2009) should be pursued in concert with investigations of the neurotrophic changes present in the respective target tissues.

References

Aksay E, Gamkrelidze G, Seung HS, Baker R, Tank DW (2001) *In vivo* intracellular recording and perturbation of persistent activity in a neural integrator. Nat Neurosci 4:184–193.

Andreassen CS, Jakobsen J, Flyvbjerg A, Andersen H (2009) Expression of

neurotrophic factors in diabetic muscle, relation to neuropathy and muscle strength. Brain 132:2724–2733.
Baker R, Delgado-García JM, McCrea R (1981) Morphological and physiological effects of axotomy on cat abducens motoneurons. In: Lesion-induced neuronal plasticity in sensorimotor systems (Flohr H, Precht W, eds), pp 51–63. Berlin: Springer.
Benítez-Temiño B, Morcuende S, Mentis GZ, de la Cruz RR, Pastor AM (2004) Expression of Trk receptors in the oculomotor system of the adult cat. J Comp Neurol 473:538–552.
Benítez-Temiño B, de la Cruz RR, Tena JJ, Pastor AM (2005) Cerebellar grafting in the oculomotor system as a model to study target influence on adult neurons. Brain Res Brain Res Rev 49:317–329.
Berardi N, Pizzorusso T, Ratto GM, Maffei L (2003) Molecular basis of plasticity in the visual cortex. Trends Neurosci 26:369–378.
Bozdagi O, Rich E, Tronel S, Sadahiro M, Patterson K, Shapiro ML, Alberini CM, Huntley GW, Salton SR (2008) The neurotrophin-inducible gene Vgf regulates hippocampal function and behavior through a brain-derived neurotrophic factor-dependent mechanism. J Neurosci 28:9857–9869.
Bradford MM (1976) A rapid and sensitive method for the quantitation of microgram quantities of protein utilizing the principle of protein-dye binding. Anal Biochem 72:248–254.
Brännström T, Kellerth JO (1999) Recovery of synapses in axotomized adult cat spinal motoneurons after reinnervation into muscle. Exp Brain Res 125:19–27.
Buttigieg H, Kawaja MD, Fahnestock M (2007) Neurotrophic activity of proNGF in vivo. Exp Neurol 204:832–835.
Büttner U, Büttner-Ennever JA (2006) Present concepts of oculomotor organization. In: Neuroanatomy of the oculomotor system (Büttner-Ennever JA, ed.), pp 1–42. Amsterdam: Elsevier.
Caleo M, Medini P, von Bartheld CS, Maffei L (2003) Provision of brain-derived neurotrophic factor via anterograde transport from the eye preserves the physiological responses of axotomized geniculate neurons. J Neurosci 23:287–296.
Calvin WH, Stevens CF (1968) Synaptic noise and other sources of randomness in motoneuron interspike intervals. J Neurophysiol 31:574–587.
Chao MV (2003) Neurotrophins and their receptors: a convergence point for many signalling pathways. Nat Rev Neurosci 4:299–309.
Cotrufo T, Viegi A, Berardi N, Bozzi Y, Mascia L, Maffei L (2003) Effects of neurotrophins on synaptic protein expression in the visual cortex of dark-reared rats. J Neurosci 23:3566–3571.
Cui Q, Tang LS, Hu B, So KF, Yip HK (2002) Expression of TrkA, TrkB, and TrkC in injured and regenerating retinal ganglion cells of adult rats. Invest Ophthalmol Vis Sci 43:1954–1964.
Davis-López de Carrizosa MA, Tena JJ, Benítez-Temiño B, Morado-Díaz CJ, Pastor ÁM, de la Cruz RR (2008) A chronically implantable device for the controlled delivery of substances, and stimulation and recording of activity in severed nerves. J Neurosci Methods 167:302–309.
Davis-López de Carrizosa MA, Morado-Díaz CJ, Tena JJ, Benítez-Temiño B, Pecero ML, Morcuende SR, de la Cruz RR, Pastor AM (2009) Complementary actions of BDNF and neurotrophin-3 on the firing patterns and synaptic composition of motoneurons. J Neurosci 29:575–587.
de la Cruz RR, Pastor AM, Delgado-García JM (1996) Influence of the postsynaptic target on the functional properties of neurons in the adult mammalian central nervous system. Rev Neurosci 7:115–149.
Delgado-García JM, del Pozo F, Baker R (1986) Behavior of neurons in the abducens nucleus of the alert cat. I. Motoneurons. Neuroscience 17:929–952.
Delgado-García JM, del Pozo F, Spencer RF, Baker R (1988) Behavior of neurons in the abducens nucleus of the alert cat. III. Axotomized motoneurons. Neuroscience 24:143–160.
Deponti D, Buono R, Catanzaro G, De Palma C, Longhi R, Meneveri R, Bresolin N, Bassi MT, Cossu G, Clementi E, Brunelli S (2009) The low-affinity receptor for neurotrophins p75 ^{NTR} plays a key role for satellite cell function in muscle repair acting via RhoA. Mol Biol Cell 20:3620–3627.
Ebendal T, Larhammar D, Persson H (1986) Structure and expression of the chicken beta nerve growth factor gene. EMBO J 5:1483–1487.
Ernfors P, Henschen A, Olson L, Persson H (1989) Expression of nerve growth factor mRNA is developmentally regulated and increased after axotomy in rat spinal cord motoneurons. Neuron 2:1605–1613.
Ernfors P, Wetmore C, Eriksdotter-Nilsson M, Bygdeman M, Strömberg I, Olson L, Persson H (1991) The nerve growth factor receptor gene is expressed in both neuronal and non-neuronal tissues in the human fetus. Int J Dev Neurosci 9:57–66.
Ferri CC, Ghasemlou N, Bisby MA, Kawaja MD (2002) Nerve growth factor alters p75 neurotrophin receptor-induced effects in mouse facial motoneurons following axotomy. Brain Res 950:180–185.
Ferrucci M, Spalloni A, Bartalucci A, Cantafora E, Fulceri F, Nutini M, Longone P, Paparelli A, Fornai F (2010) A systematic study of brainstem motor nuclei in a mouse model of ALS, the effects of lithium. Neurobiol Dis 37:370–383.
Fuchs AF, Robinson DA (1966) A method for measuring horizontal and vertical eye movement chronically in the monkey. J Appl Physiol 21:1068–1070.
González-Forero D, Alvarez FJ, de la Cruz RR, Delgado-García JM, Pastor AM (2002) Influence of afferent synaptic innervation on the discharge variability of cat abducens motoneurons. J Physiol 541:283–299.
González-Forero D, Pastor AM, Delgado-García JM, de la Cruz RR, Alvarez FJ (2004) Synaptic structural modification following changes in activity induced by tetanus neurotoxin in cat abducens neurons. J Comp Neurol 471:201–218.
Hazari MS, Pan JH, Myers AC (2007) Nerve growth factor acutely potentiates synaptic transmission in vitro and induces dendritic growth in vivo on adult neurons in airway parasympathetic ganglia. Am J Physiol Lung Cell Mol Physiol 292:L992–L1001.
Henderson CE, Camu W, Mettling C, Gouin A, Poulsen K, Karihaloo M, Rullamas J, Evans T, McMahon SB, Armanini MP, Berkemeier L, Phillips HS, Rosenthal A (1993) Neurotrophins promote motor neuron survival and are present in embryonic limb bud. Nature 363:266–270.
Huh CY, Danik M, Manseau F, Trudeau LE, Williams S (2008) Chronic exposure to nerve growth factor increases acetylcholine and glutamate release from cholinergic neurons of the rat medial septum and diagonal band of Broca via mechanisms mediated by p75NTR. J Neurosci 28:1404–1409.
Ieda M, Fukuda K (2009) New aspects for the treatment of cardiac diseases based on the diversity of functional controls on cardiac muscles: the regulatory mechanisms of cardiac innervation and their critical roles in cardiac performance. J Pharmacol Sci 109:348–353.
Ip FC, Cheung J, Ip NY (2001) The expression profiles of neurotrophins and their receptors in rat and chicken tissues during development. Neurosci Lett 301:107–110.
Johnson H, Hökfelt T, Ulfhake B (1999) Expression of p75(NTR), TrkB and TrkC in nonmanipulated and axotomized motoneurons of aged rats. Brain Res Mol Brain Res 69:21–34.
Koliatsos VE, Clatterbuck RE, Winslow JW, Cayouette MH, Price DL (1993) Evidence that brain-derived neurotrophic factor is a trophic factor for motor neurons in vivo. Neuron 10:359–367.
Küst BM, Copray JC, Brouwer N, Troost D, Boddeke HW (2002) Elevated levels of neurotrophins in human biceps brachii tissue of amyotrophic lateral sclerosis. Exp Neurol 177:419–427.
Lampl I, Reichova I, Ferster D (1999) Synchronous membrane potential fluctuations in neurons of the cat visual cortex. Neuron 22:361–374.
Lindsay RM (1994) Trophic protection of motor neurons: clinical potential in motor neuron diseases. J Neurol 242:S8–S11.
Lucidi-Phillipi CA, Clary DO, Reichardt LF, Gage FH (1996) TrkA activation is sufficient to rescue axotomized cholinergic neurons. Neuron 16:653–663.
Luther JA, Birren SJ (2009) p75 and TrkA signaling regulates sympathetic neuronal firing patterns via differential modulation of voltage-gated currents. J Neurosci 29:5411–5424.
McAllister AK, Katz LC, Lo DC (1999) Neurotrophins and synaptic plasticity. Annu Rev Neurosci 22:295–318.
Mendell LM, Arvanian VL (2002) Diversity of neurotrophin action in the postnatal spinal cord. Brain Res Brain Res Rev 40:230–239.
Merlio JP, Ernfors P, Jaber M, Persson H (1992) Molecular cloning of rat *trk*C and distribution of cells expressing messenger RNAs for members of the *trk* family in the rat central nervous system. Neuroscience 51:513–532.
Nelson SB, Turrigiano GG (2008) Strength through diversity. Neuron 60:477–482.
Nieto-Gonzalez JL, Carrascal L, Nunez-Abades P, Torres B (2009) Muscarinic modulation of recruitment threshold and firing rate in rat oculomotor nucleus motoneurons. J Neurophysiol 101:100–111.
Nishio T, Sunohara N, Furukawa S (1998) Neurotrophin switching in spinal motoneurons of amyotrophic lateral sclerosis. Neuroreport 11:1661–1665.
Obál I, Engelhardt JI, Siklós L (2006) Axotomy induces contrasting changes

in calcium and calcium-binding proteins in oculomotor and hypoglossal nuclei of BALB/c mice. J Comp Neurol 499:17–32.
Omura T, Sano M, Omura K, Hasegawa T, Doi M, Sawada T, Nagano A (2005) Different expressions of BDNF, NT3, and NT4 in muscle and nerve alter various types of peripheral nerve injuries. J Peripher Nerv Sys 10:293–300.
Palop JJ, Chin J, Roberson ED, Wang J, Thwin MT, Bien-Ly N, Yoo J, Ho KO, Yu GQ, Kreitzer A, Finkbeiner S, Noebels JL, Mucke L (2007) Aberrant excitatory neuronal activity and compensatory remodeling of inhibitory hippocampal circuits in mouse models of Alzheimer's disease. Neuron 55:697–711.
Pastor AM, González-Forero D (2003) Recruitment order of cat abducens motoneurons and internuclear neurons. J Neurophysiol 90:2240–2252.
Pastor AM, Moreno-López B, de la Cruz RR, Delgado-García JM (1997) Effects of botulinum neurotoxin type A on abducens motoneurons in the cat: ultrastructural and synaptic alterations. Neuroscience 81:457–478.
Piehl F, Frisén J, Risling M, Hökfelt T, Cullheim S (1994) Increased TrkB mRNA expression by axotomized motoneurons. Neuroreport 5:697–700.
Pinter MJ, Vanden Noven S (1989) Effects of preventing reinnervation on axotomized spinal motoneurons in the cat. I. Motoneuron electrical properties. J Neurophysiol 62:311–324.
Pizzorusso T, Berardi N, Rossi FM, Viegi A, Venstrom K, Reichardt LF, Maffei L (1999) TrkA activation in the rat visual cortex by antirat TrkA IgG prevents the effect of monocular deprivation. Eur J Neurosci 11:204–212.
Powers RK, Binder MD (2000) Relationship between the time course of the afterhyperpolarization and discharge variability in cat spinal motoneurones. J Physiol 528:131–150.
Ramaswamy S, Soderstrom KE, Kordower JH (2009) Trophic factors therapy in Parkinson's disease. Prog Brain Res 175:201–216.
Rankin SL, Guy CS, Rahimtula M, Mearow KM (2008) Neurotrophin-induced upregulation of p75NTR via a protein kinase C-delta-dependent mechanism. Brain Res 1217:10–24.
Rattiner LM, Davis M, French CT, Ressler KJ (2004) Brain-derived neurotrophic factor and tyrosine kinase receptor B involvement in amygdala-dependent fear conditioning. J Neurosci 24:4796–4806.
Rutherford LC, DeWan A, Lauer HM, Turrigiano GG (1997) Brain-derived neurotrophic factor mediates the activity-dependent regulation of inhibition in neocortical neurons. J Neurosci 17:4527–4535.
Salama-Cohen P, Arévalo MA, Grantyn R, Rodríguez-Tébar A (2006) Notch and GF/p75NTR control dendrite morphology and the balance of excitatory/inhibitory synaptic input to hippocampal neurones through Neurogenin 3. J Neurochem 97:1269–1278.
Shadlen MN, Newsome WT (1998) The variable discharge of cortical neurons: implications for connectivity, computation, and information coding. J Neurosci 18:3870–3896.
Sherwood NT, Lo DC (1999) Long-term enhancement of central synaptic transmission by chronic brain-derived neurotrophic factor treatment. J Neurosci 19:7025–7036.
Shu X, Mendell LM (1999) Nerve growth factor acutely sensitizes the response of adult rat sensory neurons to capsaicin. Neurosci Lett 274:159–162.
Singh B, Henneberger C, Betances D, Arevalo MA, Rodríguez-Tébar A, Meier JC, Grantyn R (2006) Altered balance of glutamatergic/GABAergic synaptic input and associated changes in dendrite morphology after BDNF expression in BDNF-deficient hippocampal neurons. J Neurosci 26:7189–7200.
Sumner BE (1975) A quantitative analysis of boutons with different types of synapse in normal and injured hypoglossal nuclei. Exp Neurol 49:406–417.
Tapley P, Lamballe F, Barbacid M (1992) K252a is a selective inhibitor of the tyrosine protein kinase activity of the Trk family of oncogenes and neurotrophin receptors. Oncogene 7:371–381.
Tarsa L, Balkowiec A (2009) Nerve growth factor regulates synaptophysin expression in developing trigeminal ganglion neurons in vitro. Neuropeptides 43:47–52.
Toti P, Villanova M, Vatti R, Schuerfeld K, Stumpo M, Barbagli L, Malandrini A, Costantini M (2003) Nerve growth factor expression in human dystrophic muscles. Muscle Nerve 27:370–373.
Villa AE, Bajo Lorenzana VM, Vantini G (1996) Nerve growth factor modulates information processing in the auditory thalamus. Brain Res Bull 39:139–147.
Weskamp G, Reichardt LF (1991) Evidence that biological activity of NGF is mediated through a novel subclass of high affinity receptors. Neuron 6:649–663.
Wu CW, Yeh HH (2005) Nerve growth factor rapidly increases muscarinic tone in mouse medial septum/diagonal band of Broca. J Neurosci 25:4232–4242.
Yuan Q, Hu B, So KF, Wu W (2006) Age-related reexpression of p75 in axotomized motoneurons. Neuroreport 17:711–715.
Zhang YH, Nicol GD (2004) NGF-mediated sensitization of the excitability of rat sensory neurons is prevented by a blocking antibody to the p75 neurotrophin receptor. Neurosci Lett 366:187–192.
Zhang YH, Vasko MR, Nicol GD (2002) Ceramide, a putative second messenger for nerve growth factor, modulates the TTX-resistant Na^+ current and delayed rectifier K^+ current in rat sensory neurons. J Physiol 544: 385–402.